XMM-NEWTON OBSERVATIONS OF M31: X-RAY PROPERTIES OF RADIO SOURCES AND SNR CANDIDATES

S. Trudolyubov
Institute of Geophysics and Planetary Physics, University of California, Riverside
1432 Geology Building, Riverside, CA 92521, U.S.A.
SERGEYT@CITRUS.UCR.EDU
W. Priedhorsky
Los Alamos National Laboratory
LANL, Los Alamos, NM 87545, U.S.A.
WPRIEDHORSKY@LANL.GOV

Abstract

We present the results of the ongoing *XMM-Newton* survey of the nearby spiral galaxy M31. 17 X-ray sources detected in the survey have bright radio counterparts, and 15 X-ray sources coincide with supernova remnant (SNR) candidates from optical and radio surveys. 15 out of 17 sources with radio counterparts, not SNR candidates, have spectral properties similar to that observed for background radio galaxies/quasars or Crab-like SNRs located in M31. The remaining two sources, XMMU J004046.8+405525 and XMMU J004249.1+412407, have soft X-ray spectra, and are associated with spatially resolved Hα emission regions, which makes them two new SNR candidates in M31. The observed absorbed X-ray luminosities of SNR candidates in our sample range from $\sim 10^{35}$ to $\sim 5{\times}10^{36}$ erg s^{-1}, assuming the distance of 760 kpc. Most of the SNR candidates detected in our survey have soft X-ray spectra. The spectra of the brightest sources show presence of emission lines and can be fit by thermal plasma models with $kT \sim 0.1$–0.4 keV. The results of spectral fitting of SNR candidates suggest that most of them should be located in a relatively low density regions. We show that X-ray color-color diagrams can be useful tool for distinguishing between intrinsically hard background radio sources and Crab-like SNR and thermal SNR in M31 with soft spectra.

1 Introduction

The Andromeda galaxy (M31), the closest giant spiral galaxy to our own, is an unique object for the study

Table 1: X-ray sources coincident with radio sources not identified as SNR

Source Name XMMU J00...	Flux[a]	Radio/X-ray ID[b]
3948.2+403436	0.19±0.04	37W42
4013.9+405004	856.6±7.5	37W51, SHP67
		BL Lac
4044.0+404853	0.17±0.03	37W63, SHP90
4046.8+405525	0.72±0.11	37W64, SHP94
		SNR?
4141.2+410331	7.53±0.52	37W91, SHP119
4151.4+411439	9.31±0.51	37W95, SHP132
4152.0+405429	0.12±0.03	37W97
4220.2+412641	1.02±0.05	37W116
		RX J0042.3+4126
4249.1+412407	1.24±0.09	37W140, SNR?
4251.4+412633	0.22±0.04	37W144, 37W150
4309.8+411900	0.11 - 52.91	37W153, SHP226
		Highly variable
4326.2+411912	0.23±0.04	37W158B
4329.3+413554	0.17±0.03	37W159
4344.6+412843	1.80±0.20	37W169
4437.8+414513	7.32±0.61	37W194
4648.0+420852	10.04±0.44	37W235, SHP353

[a] – Source X-ray flux in the 0.3–10 keV energy band in units of 10^{-14} erg s^{-1} cm^{-2}.

[b] – Source identifications beginning with 37W refer to the radio sources listed in Walterbos, Brinks & Shane (1985). Identifications beginning with SHP refer to entries from *ROSAT* PSPC catalog of X-ray sources in M31 by Supper et al. (2001).

Table 2: X-ray sources identified with SNR candidates

Source Name XMMU J00...	L_X^a(0.3–10 keV) $\times 10^{35}$ erg s^{-1}	Identification^b
3945.1+402950	1.74±0.28	MA 1-001
4005.1+403017	3.31±0.90	MA 2-002
4052.5+403626	7.22±1.36	MA 3-027
4110.6+404716	0.82±0.20	MA 2-013
4115.6+405741	1.45±0.36	MA 2-016
4134.8+410659	6.43±0.83	BW53
4253.6+412551	34.47±1.37	BW55
4310.6+413853	0.96±0.21	BW6
4327.9+411828	48.26±1.14	BW56,MA 2-043
4339.1+412655	18.98±0.74	BW57,MA 3-069
4353.7+411206	6.22±1.13	BW9
4447.1+412917	1.07±0.25	BW29
4451.1+412907	9.30±0.80	BW33
4452.7+415457	2.02±0.51	BW34
4514.0+413614	9.13±0.70	BW39,MA 2-048

^{a} – X-ray luminosity of the source assuming a distance of 760 kpc.

^{b} – Source identifications beginning with BW refer to the SNR candidates listed in Braun & Walterbos (1993). Identifications beginning with MA refer to the SNR candidates from Magnier et al. (1995).

Table 3: Spectral fit results for six brightest X-ray sources identified with radio-emitting objects (*XMM-Newton* EPIC data, absorbed simple power law model, 0.3–10.0 keV energy range

Source Name XMMU J00...	Photon Index	N_H^a	Flux^b
4013.9+405004	2.05±0.03	0.47±0.01	85.66±0.75
4141.2+410331	1.60±0.13	$0.15^{+0.05}_{-0.04}$	0.75±0.05
4151.4+411439	$1.89^{+0.15}_{-0.13}$	0.17±0.04	0.93±0.05
4309.8+411900	1.80±0.04	0.15±0.01	5.29±0.09
4437.8+414513	$2.15^{+0.11}_{-0.13}$	$0.17^{+0.03}_{-0.04}$	0.73±0.06
4648.0+420852	$1.86^{+0.10}_{-0.12}$	$0.40^{+0.10}_{-0.05}$	1.00±0.04

^{a} – Equivalent hydrogen absorbing column in units of 10^{22} cm^{-2}.

^{b} – Source X-ray flux in the 0.3–10 keV energy band in units of 10^{-13} erg s^{-1} cm^{-2}

of optical and X-ray astronomy. Its proximity and favorable orientation allow to observe stellar populations over the full extent of the galaxy at a nearly uniform distance, and with less severe effects of line-of-sight contamination from interstellar gas and dust. Due

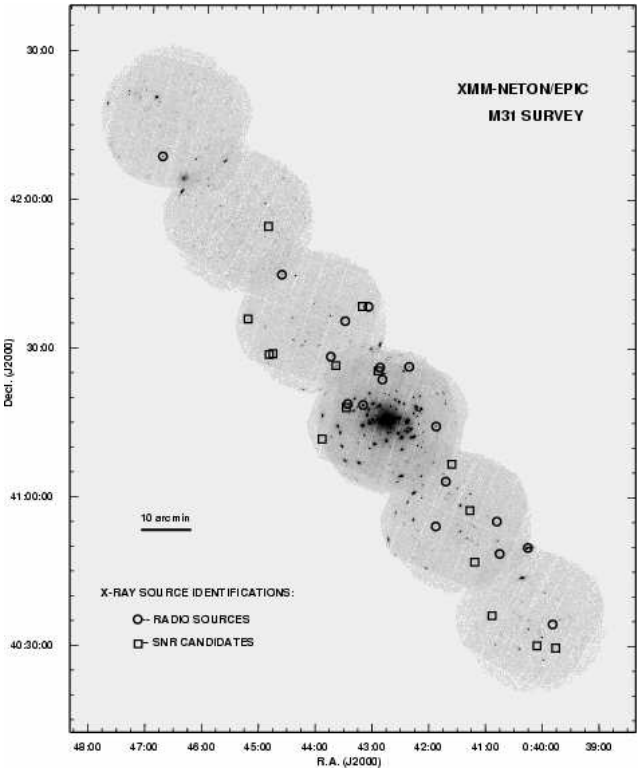

Figure 1: *XMM-Newton* EPIC X-ray image of M31 in the 0.3–10 keV energy range. X-ray sources identified with radio sources and SNR candidates are marked by *circles* and *squares*.

to similarities between the two galaxies, the results from the study of M31 provide an important benchmark for comparison with the results from the study of our own Milky Way galaxy. M31 was observed extensively in X-rays. *EINSTEIN*, *ROSAT*, *Chandra* and *XMM-Newton* missions detected hundreds of sources, with some bright X-ray sources coincident with radio-emitting sources and SNR candidates from optical surveys. In the extensive *ROSAT* PSPC survey of M31 (Supper et al. 2001), 16 X-ray emitting SNR were identified. Recently, Kong et al. (2003) identified two new SNRs using the data of *Chandra* and Very Large Array (VLA) observations. Trudolyubov et al. (2004) used *XMM-Newton* observations to study X-ray spectral properties of the 3 bright thermal SNR in the northern disk of M31.

2 Source identification and classification

Using the data of the *XMM-Newton* survey of M31, we detected about 600 X-ray point sources in the six *XMM-Newton* fields covering the major axis of M31. We searched for radio, optical and X-ray counterparts

to the *XMM-Newton* sources using the existing catalogs and images from the CTIO/KPNO Local Group Survey (LGS) (Massey et al. 2001). We varied the search radius based on both the accuracy of the catalogs and localization errors of *XMM-Newton* sources (upper limit of 5 arcseconds). We used the following catalogs and corresponding search radii:

Radio sources: VLA All-sky Survey Catalog (Condon et al. 1998) and the lists of Walterbos, Brinks & Shane (1985) and Braun (1990) – 5 arcsecond search radius. 17 X-ray sources were found to coincide with radio sources.

Supernova remnant candidates: the lists by Braun & Walterbos (1993) and Magnier et al. (1995) – 10 arcsecond search radius. 15 X-ray sources have SNR counterparts in M31.

X-ray sources: the *ROSAT* PSPC catalog of sources in the field of M31 (Supper et al. 2001) – search radius specified by position accuracy for each individual source.

The information on the positions and identifications of the X-ray sources coincident with radio sources and SNR candidates is shown in Table 1 and 2. The *XMM-Newton* EPIC X-ray images of M31 with source positions marked are shown in Fig. 1.

3 Radio sources

17 bright *XMM-Newton* sources not identified as SNR candidates coincide with bright radio sources detected with the VLA all-sky (Condon et al. 1998) and earlier surveys (Walterbos, Brinks & Shane 1985; Braun 1990). 15 out of 17 sources with radio counterparts have spectral properties similar to that observed for background radio galaxies/quasars and Crab-like SNR in M31. The brightest objects have X-ray spectra well presented by absorbed power laws with indices between $\sim$ 1.6 and $\sim$ 2.2, typical for this source class (Table 3; Fig. 2). For the majority of bright radio sources the corresponding values of the interstellar absorption inferred from their X-ray spectra are well above the expected Galactic value in the direction of M31 (Dickey & Lockman 1990), supporting their identification with objects in the background of M31.

Two *XMM-Newton* sources, identified with radio-emitting objects, have soft X-ray spectra. The X-ray spectrum of the first source, XMMU J004046.8+405525, can be well fit to the absorbed Raymond-Smith (RS) thermal plasma emission model

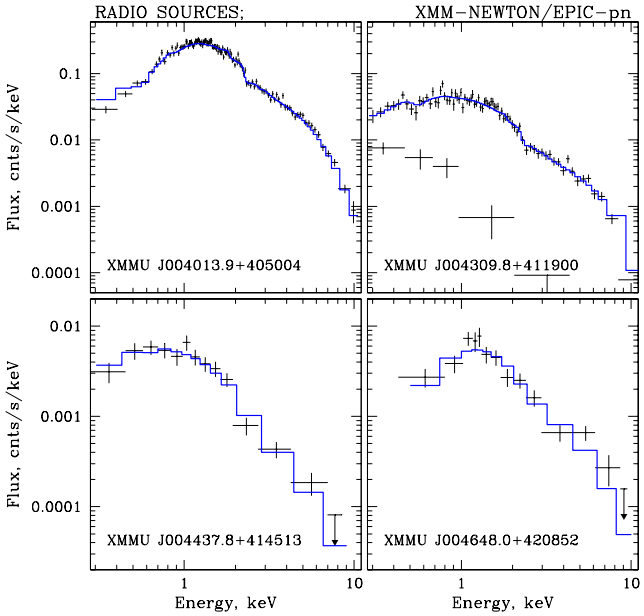

Figure 2: EPIC-pn count spectra of the four brightest X-ray sources coincident with radio sources. For each spectrum the absorbed power law model fits are shown with *blue solid* histograms. The spectra of a variable source XMMU J004309.8+411900, corresponding to the high and low levels of X-ray flux are shown in the *upper right* panel.

with $kT \sim 0.2$ keV. The corresponding absorbed source luminosity in the 0.3–3 keV energy band is $\sim 5{\times}10^{35}$ erg s^{-1} assuming the distance of 760 kpc. The other source, XMMU J004249.1+412407, has a spectrum well approximated by the absorbed RS model with $kT \sim 0.4$ keV and luminosity of $\sim 9{\times}10^{35}$ erg s^{-1} in the 0.3–3 keV energy range. The inspection of the optical LGS images of M31 revealed two spatially resolved Hα emission regions, coincident with these two X-ray sources (Fig. 3, 4). The combination of the soft thermal X-ray spectra, extended Hα and bright radio counterparts allows to propose XMMU J004046.8+405525 and XMMU J004249.1+412407 as new SNR candidates in M31.

4 Supernova remnant candidates

15 *XMM-Newton* sources detected in M31 fields were identified with SNR candidates from optical surveys (Braun & Walterbos 1993; Magnier et al. 1995). Most of these sources were previously detected with *ROSAT* and identified as SNR (Supper et al. 2001; Magnier et al. 1997).

All relatively bright SNR candidates have relatively soft X-ray spectra (Fig. 5). We fitted the spectra of

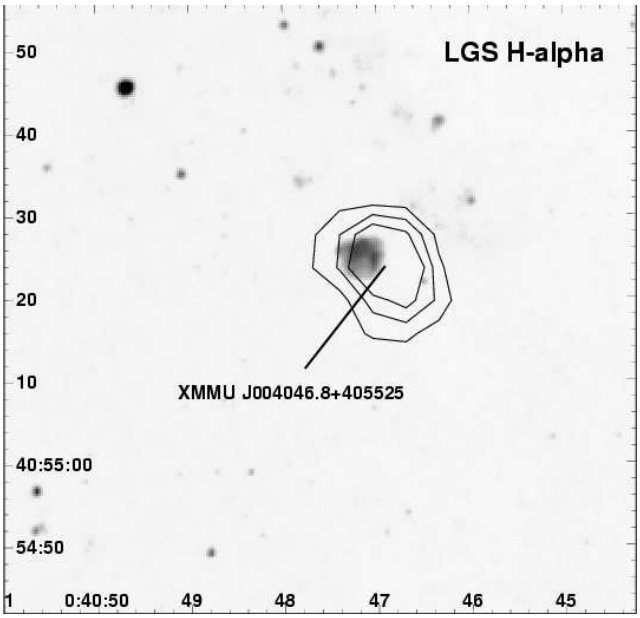

Figure 3: Optical Hα image of the southern disk of M31 from the Local Group Survey (Massey et al. 2001) with *XMM-Newton* EPIC X-ray contours overlaid. The image shows spatially resolved Hα region, associated with the soft X-ray source XMMU J004046.8+405525 and radio sources 37W64 from Walterbos, Brinks and Shane (1985) and GLG068 from Gelfand et al. (2005).

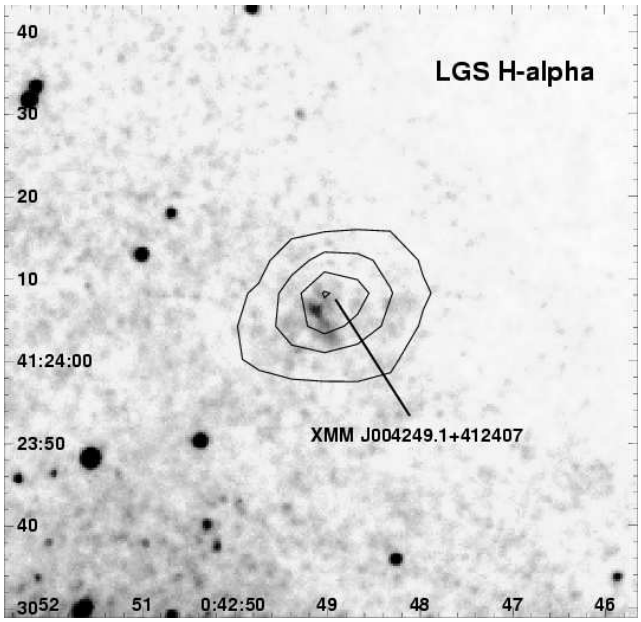

Figure 4: Optical Hα image of the southern disk of M31 from the Local Group Survey (Massey et al. 2001) with *XMM-Newton* EPIC X-ray contours overlaid. The image shows spatially resolved Hα region, associated with the soft X-ray source XMMU J004249.1+412407 and radio source 37W140 from Walterbos, Brinks and Shane (1985).

SNR candidates with various single component spectral models including a simple power law, thermal bremsstrahlung, black body, RS thermal plasma, and non-equilibrium ionization collisional plasma (NEI) models with interstellar absorption. RS models with characteristic temperatures of 0.1–0.4 keV and NEI models with temperatures of 0.5–1.5 keV give the best approximation to the data for 6 bright SNR candidate sources (Fig. 5). The absorbed X-ray luminosities of SNR candidates range from $\sim 10^{35}$ to $\sim 5{\times}10^{36}$ erg s^{-1} assuming the distance of 760 kpc. The estimated ages of SNR range from $\sim$ 2000 to 20,000 years and the number density of ambient gas is $\sim$ 0.005–0.4 cm^{-3}, suggesting that these SNR may be located in a relatively low density regions. The X-ray measured chemical abundances were found to be similar to their optically determined values (Blair, Kirshner & Chevalier 1982).

5 X-ray color-color diagram

In order to facilitate comparison between spectral properties of the radio sources and SNR candidates detected in our survey, we constructed their X-ray color-color diagram. We calculated the total number of counts for each source using its corrected EPIC-pn spectra in three energy bands: the soft band (0.3–1.0 keV), medium band (1.0–2.0 keV) and hard band (2.0–7.0 keV). Two X-ray colors were defined for each source as: HR1 = $(S - M)/T$ (soft color) and HR2 = $(H - M)/T$ (hard color), where S, M, and H are the counts in soft, medium and hard bands respectively, and T is the total number of source counts in the 0.3–7.0 keV energy range. We used the data for the 16 brightest sources (10 radio sources and 6 SNR candidates), each of which provided more than 50 counts in EPIC-pn.

Figure 6 shows the X-ray color-color diagram for the bright X-ray sources identified with radio sources and SNR candidates. There are two distinct concentrations of sources in this diagram. The first group with HR1 $>$ 0.3 includes intrinsically soft sources: bright thermal SNR and two radio sources, XMMU J004046.8+405525 and XMMU J004249.1+412407. The second group includes harder radio sources. The X-ray color-color diagrams show that they can be a useful tool for distinguishing between sources with intrinsically soft and hard spectra like thermal SNR and

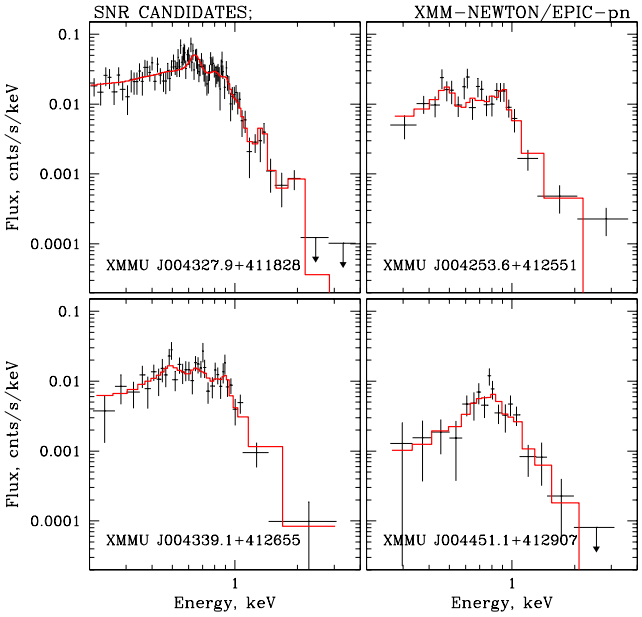

Figure 5: EPIC-pn count spectra of the four brightest SNR candidates in the 0.3–3.0 keV energy band. For each spectrum the absorbed Raymond-Smith thermal plasma model fits are shown with *red solid* histograms.

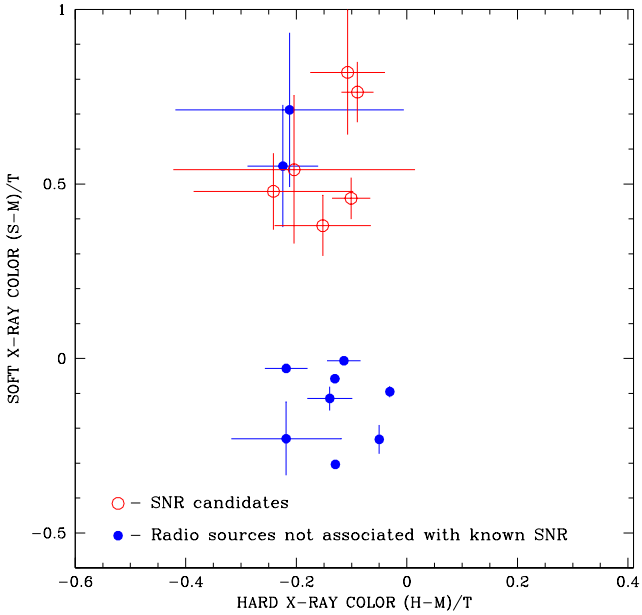

Figure 6: X-ray color-color diagram of the brightest radio sources (*blue filled circles*) and SNR candidates (*red open circles*).

background radio sources. On the other hand, this method shows no difference between Crab-like SNR and background radio sources. The combination of low-energy absorption and limited instrument bandpass also have a significant effect on the source position on the color-color diagram (Di Stefano & Kong 2003). For example, a source with an intrinsically soft spectrum, if highly absorbed, can easily "migrate" to the region on the color diagram normally occupied by sources with much harder spectra. Therefore, additional information, such as X-ray variability, luminosity and source counterparts at other wavelengths, is needed to classify the X-ray source.

6 Summary

Nearly 600 X-ray sources were detected in the ongoing *XMM-Newton* survey of M31. 17 of them have bright radio counterparts not identified with SNR candidates, and 15 sources coincide with SNR candidates from radio and optical surveys.

15 out of 17 sources with radio counterparts, not known to be SNR candidates from optical surveys, have spectral properties similar to that observed for background radio galaxies/quasars or Crab-like supernova remnants located in M31. The energy spectra of the brightest objects are well represented by an absorbed power law with photon indices between ~ 1.6 and ~ 2.2, and low-energy absorption in excess of the Galactic foreground value in the direction of M31. The remaining two sources, XMMU J004046.8+405525 and XMMU J004249.1+412407, have soft X-ray spectra, and are associated with spatially resolved Hα emission regions, which makes them two new SNR candidates in M31.

Most of the SNR candidates detected in our survey have soft X-ray spectra. The spectra of the brightest sources show presence of emission lines and can be fit by thermal plasma models with $kT \sim 0.1$–0.4 keV. The observed absorbed X-ray luminosities of our SNR candidates range from $\sim 10^{35}$ to $\sim 5\times10^{36}$ erg s^{-1}, assuming the distance of 760 kpc. The results of spectral fitting suggest that most of the bright SNR candidates in our sample may be located in the low density regions.

We show that X-ray color-color diagrams can be a useful tool for distinguishing between intrinsically hard background radio sources and Crab-like SNR and thermal SNR in M31.

Acknowledgments

Support for this work was provided through NASA *XMM-Newton* Grant NAG5-12390. *XMM-Newton* is

an ESA Science Mission with instruments and contributions directly funded by ESA Member states and the USA (NASA). This research has made use of data obtained through the High Energy Astrophysics Science Archive Research Center Online Service, provided by the NASA/Goddard Space Flight Center.

References

Blair, W. P., Kirshner, R. P., Chevalier, R. A. 1982, ApJ, 254, 50

Braun, R. 1990, A&AS, 72, 761

Braun, R., Walterbos, R. A. M. 1993, A&AS, 98, 327

Condon, J. J., Cotton, W. D., Greisen, E. W., Yin, Q. F., Perley, R. A., Taylor, G. B., Broderick, J. J. 1998, AJ, 115, 1693

Dickey, J. M., Lockman F. J. 1990, ARA&A, 28, 215

Di Stefano, R., Kong, A. K. H. 2003, ApJ, 592, 884

Gelfand, Y., Lazio, J., Gaensler, B. 2005, in *"X-ray and Radio Connections"*, eds. Sjouwerman, L. O. & Dyer, K. K., Published electronically at http://www.aoc.nrao.edu/events/xraydio

Kong, A. K. H., Sjouwerman, L. O., Williams, B. F., Garcia, M. R., Dickel, J. R. 2003, ApJ, 590, 21

Magnier, E. A., Prins, S., van Paradijs, J., Lewin, W. H. G., Supper, R., Hasinger, G., Pietsch, W., Truemper, J. 1995, A&AS, 114, 215

Magnier, E. A., Primini, F. A., Prins, S., van Paradijs, J., Lewin, W. H. G. 1997, ApJ, 490, 649

Massey. P., Hodge, P. W., Holmes, S., Jacoby, G., King, N. L., Olsen, K., Saha, A., Smith, C. 2001, in American Astronomical Society Meeting, 199, 1305

Supper, R., Hasinger, G., Lewin, W. H. G., Magnier, E. A., van Paradijs, J., Pietsch, W., Read, A. M. Truemper, J. 2001, A&A, 373, 63

Trudolyubov, S., Kotov, O., Priedhorsky, W., Cordova, F., Mason, K. 2004, ApJ, submitted (astro-ph/0401227)

Walterbos, R. A. M., Brinks, E., Shane, W. W. 1985, A&AS, 61, 451